JOURNAL OF MATERIALS SCIENCE 26 (1991) 35–42

Application of decreased hot-rolling reduction treatments for improved mechanical properties of quenched and highly-tempered low alloy structural steels

YOSHIYUKI TOMITA
Department of Metallurgical Engineering, College of Engineering, University of Osaka Prefecture, 4-804 Mozu-Umemachi Sakai, Osaka 591, Japan

Decreased hot-rolling reduction treatments from 98% ≡ ×50 elongation to 80% ≡ ×5 elongation, which modify the sulphide-inclusion shape from a stringer to an ellipse, have been applied to improve the mechanical properties of quenched and highly tempered low alloy structural steels. The decreased hot-rolling reduction treatments significantly increased the transverse fracture ductility at similar strengths and uniform elongation levels independent of the type of steel. The treatments also improved the transverse Charpy U-notch (CUN) impact energy independent of the type of steel. The effect of test temperature on CUN impact energy fell into two categories; (1) the treatments significantly improved transverse CUN impact energy in temperature regions which exhibited a ductile fracture mode, (2) the improvement in the mechanical properties was reduced when the temperature decreased and a brittle fracture mode appeared. The results are briefly discussed in terms of a model involving large voids initiated at sulphide-inclusion sites and local shear bands developed between the large voids.

1. Introduction

Commercial structural low alloy steels have generally been used for many engineering components in quenched and highly-tempered conditions. In spite of the best efforts of design engineers, the engineering components still fail in service from time to time and the failure is mainly responsible for mechanical anisotropy. Although the mechanical anisotropy occurs by microstructural banding which is a manifestation of the segregation of one or more elements, in the majority of cases it is closely associated with sulphide inclusions elongated in the rolling direction, thus the metallurgist may be required to investigate the development of the mechanical properties through modification of the sulphide-inclusion shape by an economical method. So far, considerable research effort has been directed toward modifying the inclusion shape of steels. For example, the technical importance of chemical means, i.e., the addition of calcium or rare earth elements to molten steels to modify the sulphide-inclusion shape has been reported. These methods have been reviewed by Leslie [1]. The calcium or rare earth modification is, however, generally impracticable and quite expensive in commercial practice because some difficulty may be encountered in commercial steelmaking practice: (1) the calcium element is apt to vaporize because of its low boiling point and poor solubility to the molten steel. (2) The rare earth elements are liable to react with activated oxygen [O] in the molten steel and refractory materials and atmosphere. (3) The rare earth oxide and oxysulphide accumulate at the bottom of the ingot and cause deterioration of the ductility and toughness of steel. (4) The calcium or rare earth injection into the melt in the ladle requires comparatively high technique and operating costs. In such a situation, the potential approach, which is economical in commercial practice and effective for the large-sized applications, has been suggested by the author whereby sulphide inclusions are modified and the mechanical properties are significantly improved. Most recently, the author has shown [2] that decreased hot-rolling reduction treatments from 98% ≡ ×50 elongation to 80% ≡ ×5 elongation modified the sulphide-inclusion shape from a stringer to an ellipse and improved the plane strain fracture toughness of quenched and lightly tempered structural low alloy steels. The effectiveness in improving the mechanical properties is attributed to the fact that modified sulphide inclusions act to blunt and arrest cracks propagating across the specimen which would normally cause failure, and considerably suppress lamellate fracture which occurs in a brittle manner along the interfaces of the sulphide inclusion and matrix at the crack tip.

In the present work, the decreased hot-rolling reduction treatments have been applied to improve the mechanical properties of quenched and highly tempered structural low alloy steels used as engineering components in commercial practice.

0022–2461/91 $03.00 + .12

TABLE I Chemical composition of steels used, wt%

Designation of steel	C	Si	Mn	P	S	Cr	Mo	Ni
Steel A	0.40	0.28	0.81	0.017	0.019	—	—	—
Steel B	0.40	0.26	0.72	0.016	0.021	1.10	0.25	—
Steel C	0.40	0.30	0.79	0.016	0.019	0.87	0.26	1.89
Steel D	0.40	0.34	0.79	0.008	0.001	0.85	0.26	1.87

2. Experimental procedure

Four low alloy structural steels whose chemical compositions are given in Table I were used in this investigation. Steels A, B, and C were prepared as 30×10^3 kg air-melted and vacuum-degassed heats. Their ingots (2.5×10^3 kg) were hot-rolled to two different forms at a temperature of 1473 K: (1) 80 mm diameter hot-rolled bar stock (98% ≡ × 50 elongation hot-rolling reduction) (98% HRT steel) and (2) 250 mm diameter hot-rolled bar stock (80% ≡ × 5 elongation hot-rolling reduction) (80% HRT steel). Steel D was prepared as 30×10^3 kg vacuum arc-melted heat and the ingots (2.5×10^3 kg) were hot-rolled to 80 mm diameter (98% VAR steel D). Mechanical test steels were cut in the longitudinal and transverse orientation (Fig. 1) from the bars and machined to the required dimensions. Each steel was fully annealed at 1173 K for 7.2 ksec.

The test steels were heat treated by austenitization under dynamic argon atmosphere for 7.2 ksec at a temperature of 1173 K followed by direct quenching in water (for steel A) or oil (for steels B and C). The test steels were subsequently tempered at 923 K for 7.2 ksec followed by water cooling. The mechanical properties were determined by tensile and Charpy impact tests. The tensile specimens as shown in Fig. 2a were pulled with an Instron machine at room temperature (293 K) at a constant strain rate of 6.70×10^{-4} sec^{-1}. The standard full size Charpy U-notch (CUN) impact specimens (Fig. 2b) were broken at temperature from 77 to 293 K in Charpy impact machine.

The non-metallic inclusions were identified using an electron probe microanalyser (EPMA). The volume fraction and shape of sulphide inclusions were determined at a magnification of × 400 by optical microscopy. Fracture morphology was characterized by scanning electron microscopy. Prior austenite grain size was determined by linear analysis by optical microscopy. In order to determine the affect of hot-rolling reduction on texture, (100) pole figures in the sections parallel to the rolling direction were measured by X-ray diffraction using MoKα radiation.

3. Results and discussion

3.1. Metallographic observations

Identification of non-metallic inclusions was made by EPMA and the volume fraction and their shape were determined by optical microscopy. The results are shown in Figs 3 and 4, and Table II. The results are summarized as follows. (1) The majority of the non-metallic inclusions were sulphide, i.e., MnS, independent of the type of steel (Fig. 3). (2) The volume fraction of the sulphide inclusions had similar levels independent of hot-rolling reduction for each steel. (3) The shape of the sulphide inclusions was modified from a stringer to an ellipse as hot-rolling reduction decreased from 98 to 80% independent of the type of

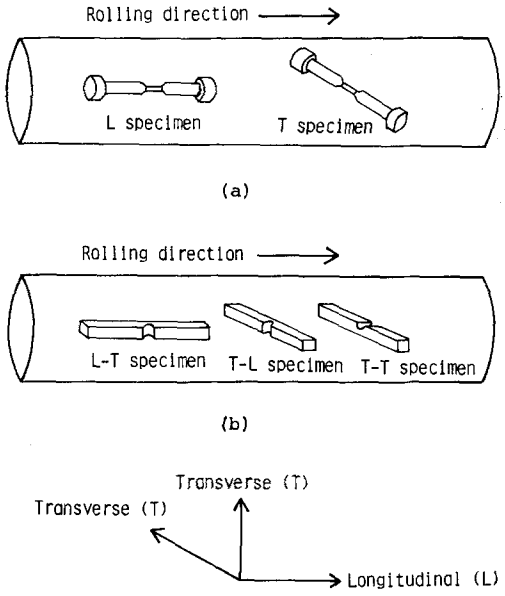

Figure 1 Test orientation of specimen. (a) tensile specimen, (b) Charpy impact specimen.

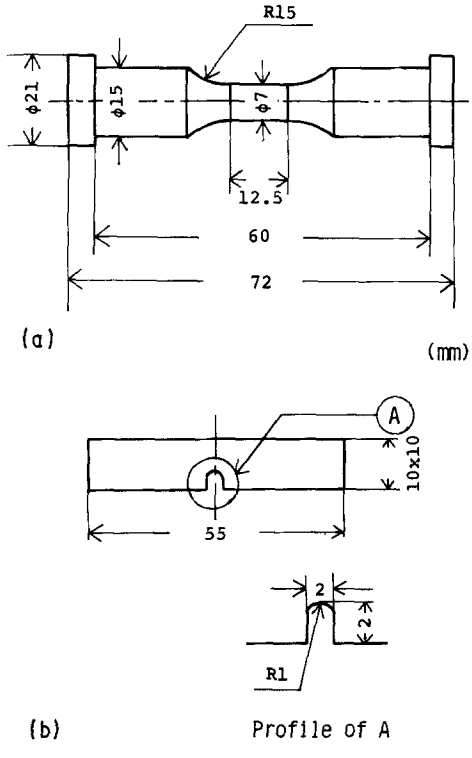

Figure 2 Shape and dimensions of test specimens. (a) tensile specimen, (b) Charpy impact specimen.

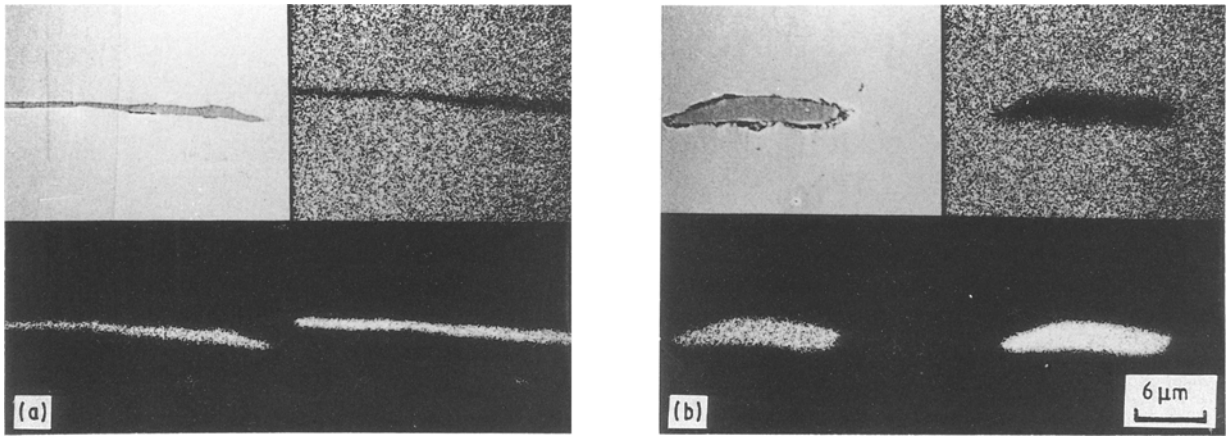

Figure 3 Example of identification of non-metallic inclusions (EPMA). (a) 98% HRT steel C, (b) 80% HRT steel C.

steel. (4) The average length of the sulphide inclusions decreased from about 50 to 27 μm when hot-rolling reduction decreased from 98% ≡ × 50 elongation (98%) to 80% ≡ × 5 elongation (80%), which, in turn, produced a corresponding increase in the average width from 2.2 to 6.2 μm. (5) The average aspect ratio of the sulphide inclusions decreased from about 17 to 4 as hot-rolling reduction decreased from 98 to 80%. (6) The difference of prior austenite grain size are not extreme. (7) There were few non-metallic inclusions for steel D. (8) Optical microscopy revealed that appreciable microstructural bands were not observed after quenching and tempering. (9) X-ray measurements revealed that the texture of {111} having a weak pole density of a maximum 1.2 (ratio to α-Fe with random direction) was observed independent of the two steels, but there was little difference in the texture between the two steels (Fig. 4).

3.2. Mechanical properties

Figs 5 to 7 show the affect of hot-rolling reduction on tensile properties for the four steels studied. The results obtained are summarized as follows. (1) 0.2% yield stress (σ_y), and true uniform strain (ε_u) are little affected by decreased hot-rolling reduction independent of steels A, B and C. (2) True strain at fracture, fracture ductility, (ε_f) in the transverse orientation was significantly improved by decreased hot-rolling reduction independent of the steels. (3) The mechanical properties of the 80% HRT steel C compared to the 98% VAR steel D were somewhat inferior.

Figs 8 to 10 show the affect of hot-rolling reduction on CUN impact properties of four steels studied. It was found from this table that CUN impact energies in the longitudinal orientation (L–T) were little influenced by decreased hot-rolling reduction independent of steels and test temperature. On the other hand,

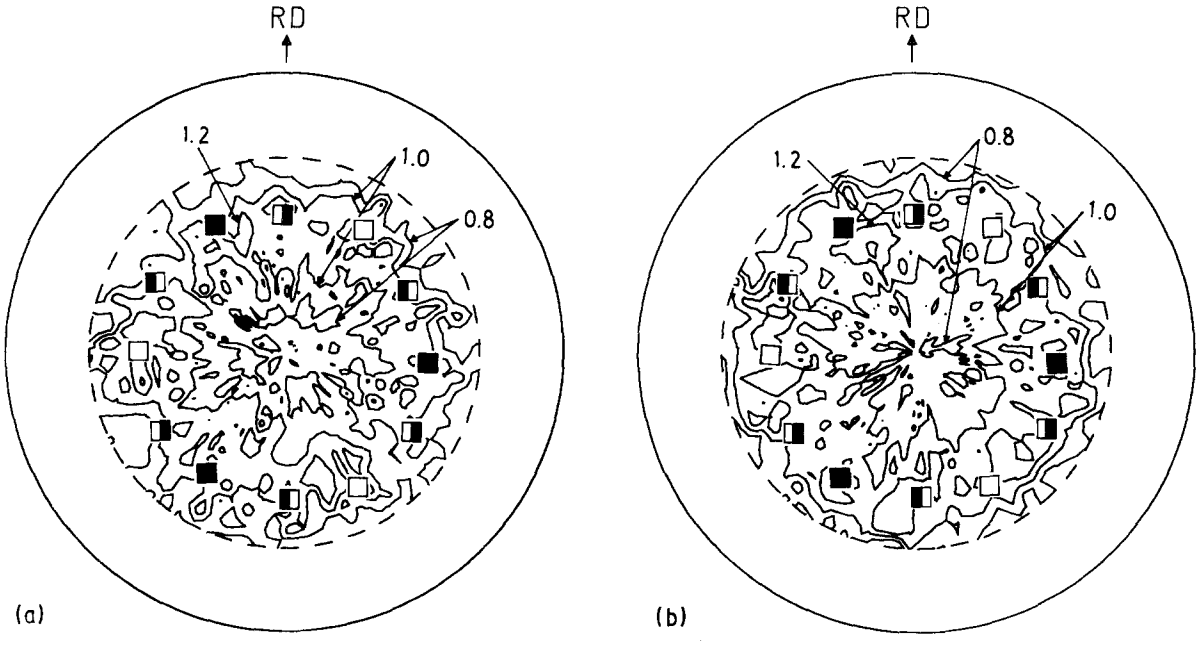

Figure 4 (100) pole figures; number indicates pole density (X-ray). (a) 98% HRT steel C, (b) 80% HRT steel C. (□ (1 1 1)[1 $\bar{1}$ 0], ■ (1 1 1)[1 $\bar{1}$ 0], □ (1 1 1)[$\bar{2}$ 1 1], □ (1 1 1)[2 $\bar{1}$ $\bar{1}$])

TABLE II Microstructural parameters of steels used

Designation of steel	Hot-rolling reduction (%)	Inclusion type	Volume fraction f(%)	Inclusion size			PAG* (μm)
				Length l(μm)	Width w(μm)	Aspect ratio l/w	
Steel A	80	MnS	0.171	27.3	6.6	4.1	19.7
	98	MnS	0.176	52.5	3.1	16.9	15.5
Steel B	80	MnS	0.168	29.9	6.9	4.3	22.3
	98	MnS	0.162	53.9	3.1	17.4	16.9
Steel C	80	MnS	0.156	25.3	6.5	3.9	21.8
	98	MnS	0.150	48.3	2.8	17.3	15.8
Steel D	98	—	—	—	—	—	14.9

*PAG; Average prior austenite grain size.

CUN impact energies in the transverse orientation (T–L and T–T) were significantly improved by decreased hot-rolling reduction. The temperature dependence of transverse CUN impact energies, however, exhibited a different response among the steels; for steel C the mechanical isotropy was somewhat improved at 77 K, but for steels B at 193 K and for steel A there was little improvement at 193 K and below. It was also found that the 80% HRT steel C compared to the 98% VAR steel D became inferior as the test temperature decreased.

3.3. Fractography

It is well known that fractography directly describes the situation of the fracture process and provides valuable evidence concerning the fracture mechanism, therefore, fractography was carried out on the fractured steel. It can be seen from the above results that the mechanical properties in the transverse orientation were significantly developed, while the mechanical properties in the longitudinal orientation were little improved. Fractography was, therefore, focused on the test specimens in the transverse orientation. Fig. 11 shows a representative fracture surface from transverse tensile specimens of steels C and 98% VAR steel D fractured at room temperature. Fractography revealed that the fracture surface contains two different types of void independent of hot-rolling reduction. The results obtained are summarized as follows.

(1) The fracture surface consisted of two types of voids – large voids that were initiated at sulphide-inclusion sites (inclusion voids) and fine voids contained between the large voids which were nucleated at carbides

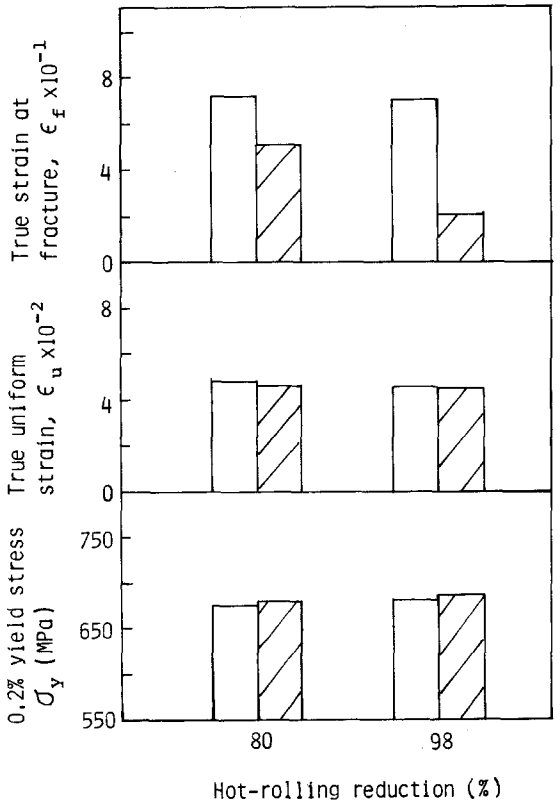

Figure 5 Effect of hot-rolling reduction on tensile properties of steel A. (□ L specimen, □ T specimen).

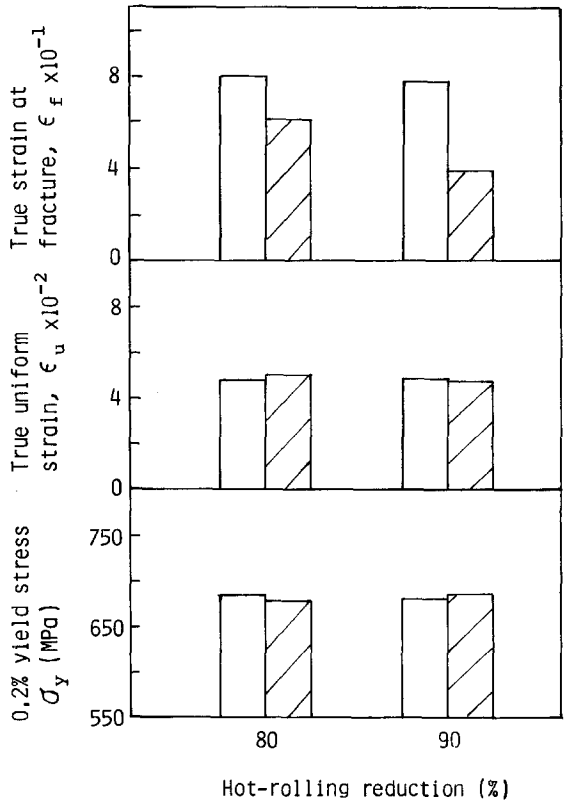

Figure 6 Effect of hot-rolling reduction on tensile properties of steel B. Symbols as in Fig. 5.

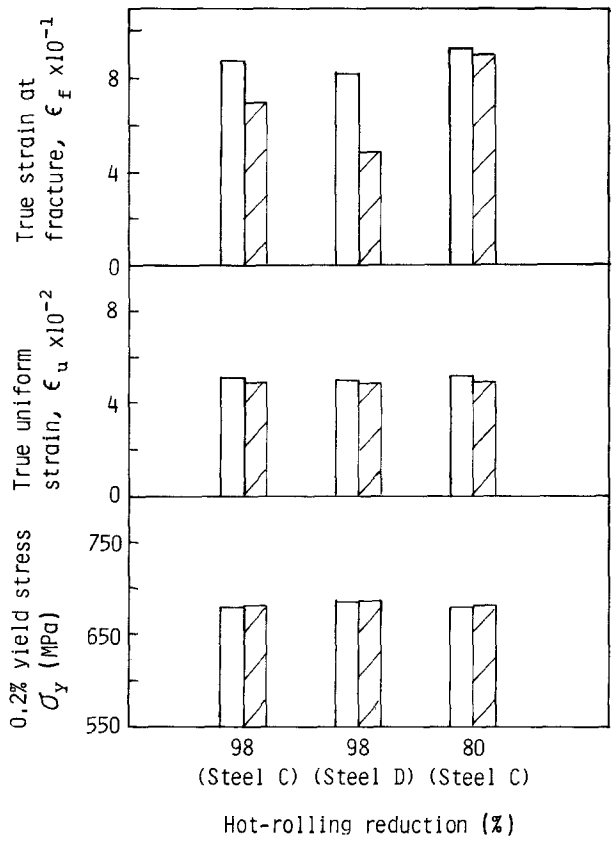

Figure 7 Effect of hot-rolling reduction on tensile properties of steels C and D. Symbols as in Fig. 5.

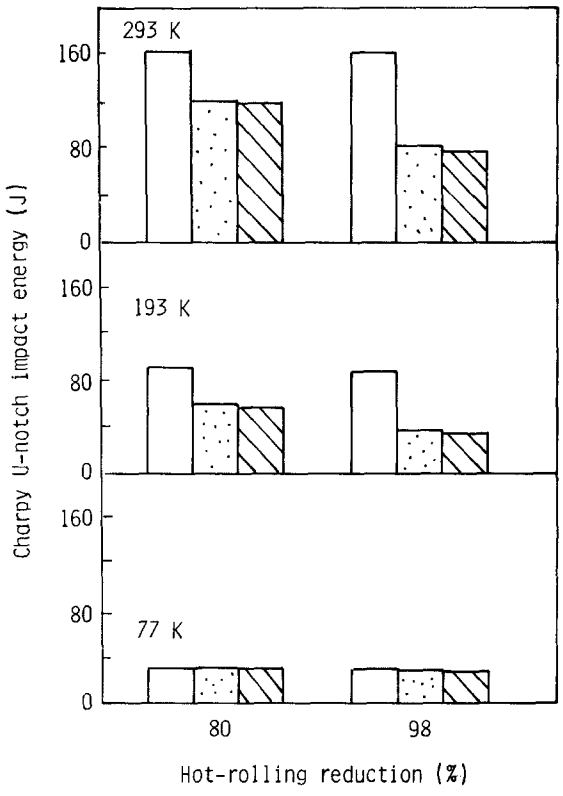

Figure 8 Effect of hot-rolling reduction on Charpy U-notch impact energy of steel A. (□ L–T specimen, ⊡ T–L specimen, ▨ T–T specimen).

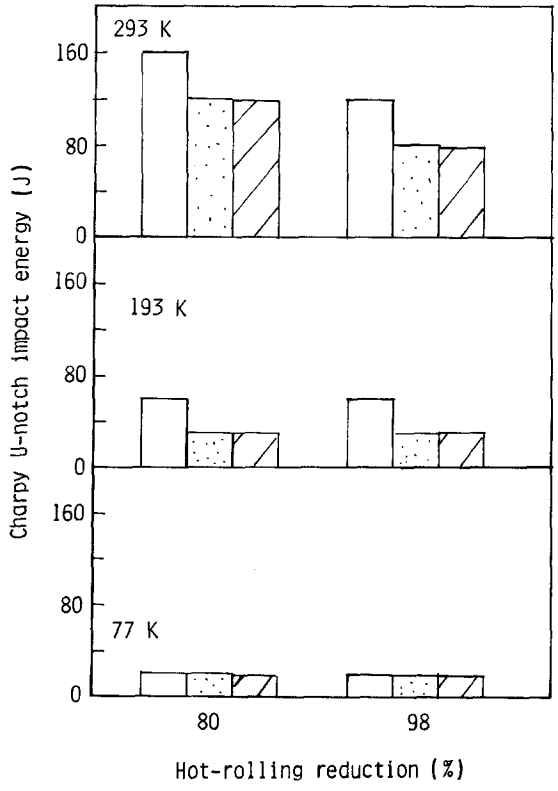

Figure 9 Effect of hot-rolling reduction on Charpy U-notch impact energy of steel B. Symbols as in Fig. 8.

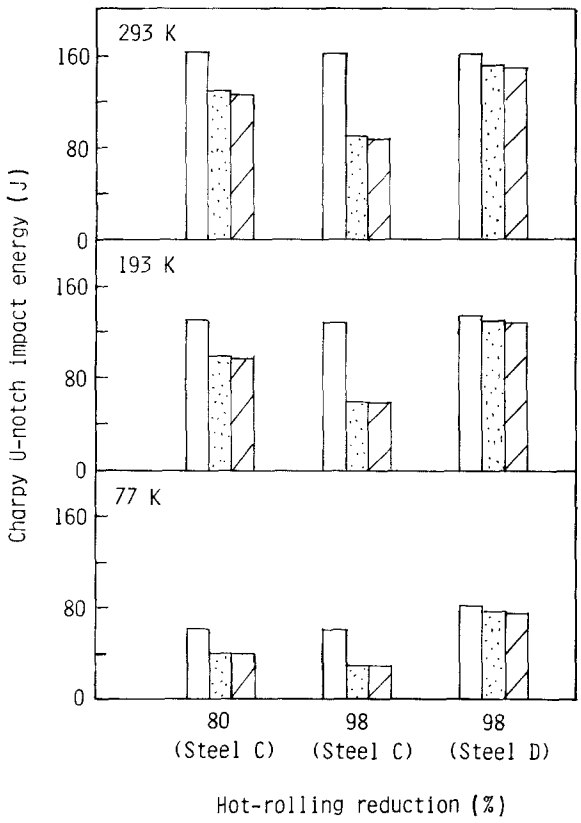

Figure 10 Effect of hot-rolling reduction on Charpy U-notch impact energy of steels C and D. Symbols as in Fig. 8.

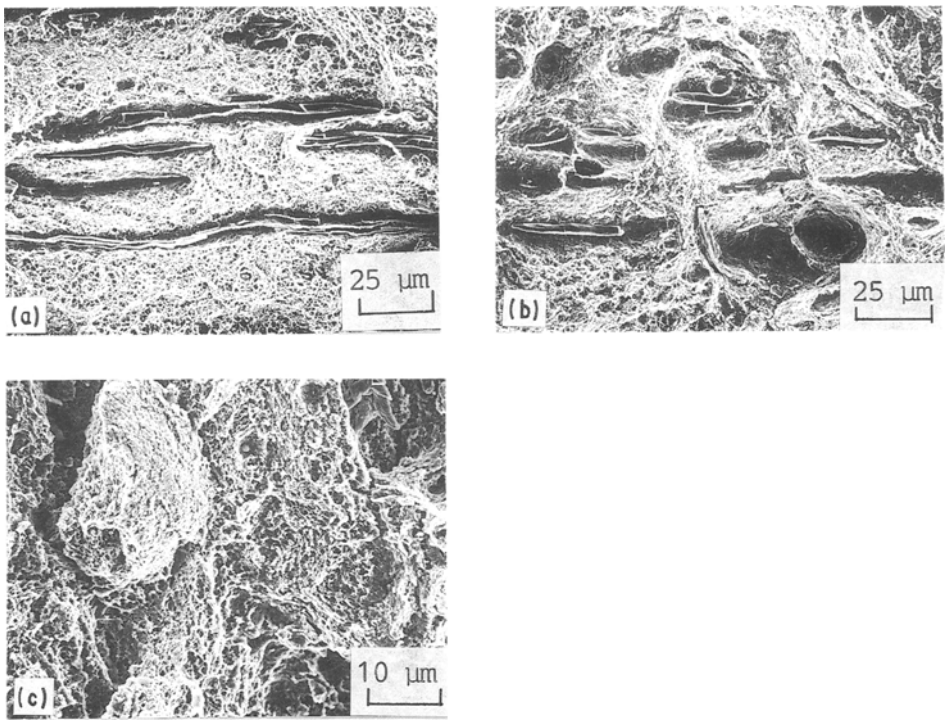

Figure 11 Fracture surface from transverse tensile specimens (SEM). (a) 98% HRT steel C, (b) 80% HRT steel C, (c) 98% VAR-steel D.

precipitated during tempering (carbide voids). (2) The inclusion voids approximately correspond to the size of the inclusions independent of hot-rolling reduction; for 98% HRT steel C the inclusion voids appeared in stringer form and for 80% HRT steel C the inclusion voids appeared in ellipse form. (3) The carbide voids of 80% HRT steel C compared to those of the 98% HRT steel C are small. (4) The fracture surface of 98% VAR steel D consisted of a well defined dimple pattern.

The fracture mode of CUN impacted T–L and T–T specimens at room temperature was investigated first. Typical results are shown in Fig. 12. The fracture surface under the U-notch consisted of inclusion voids corresponding to the size of the inclusions and carbide voids, as seen in the tensile specimens. The size of the carbide voids in the fracture surface of CUN impacted specimens compared to that in the fracture surface of tensile specimens was, however, somewhat finer because of the high strain rate. The fracture mode of

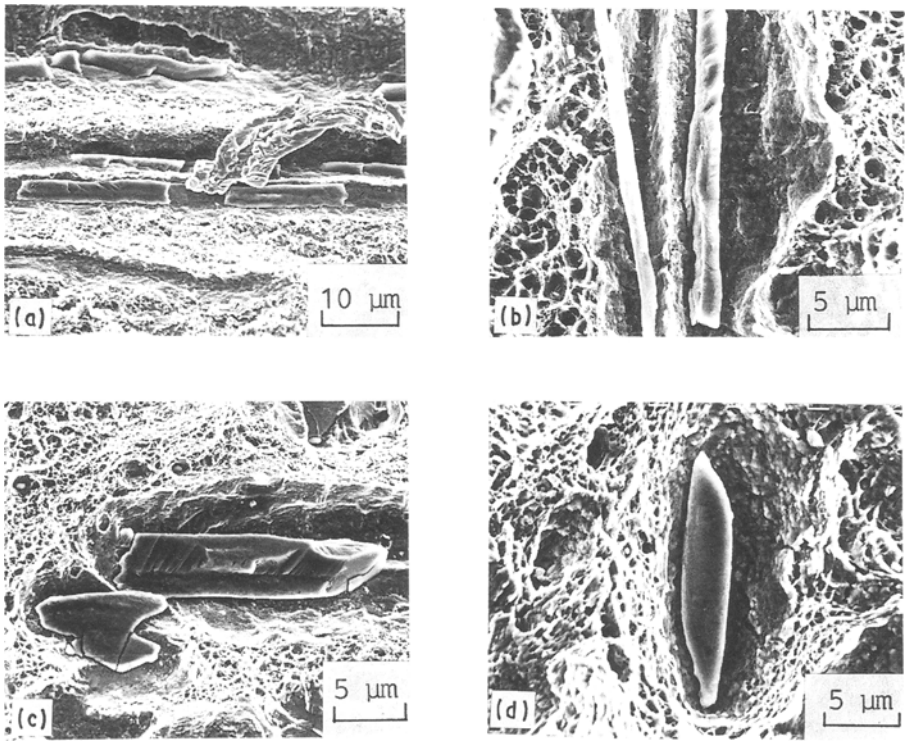

Figure 12 Fracture surface of transverse Charpy U-notch impact specimens fractured at 293 K (SEM). (a) and (b); T–L and T–T specimens for 98% HRT steel C, respectively. (c) and (d); T–L and T–T specimens for 80% HRT steel C, respectively.

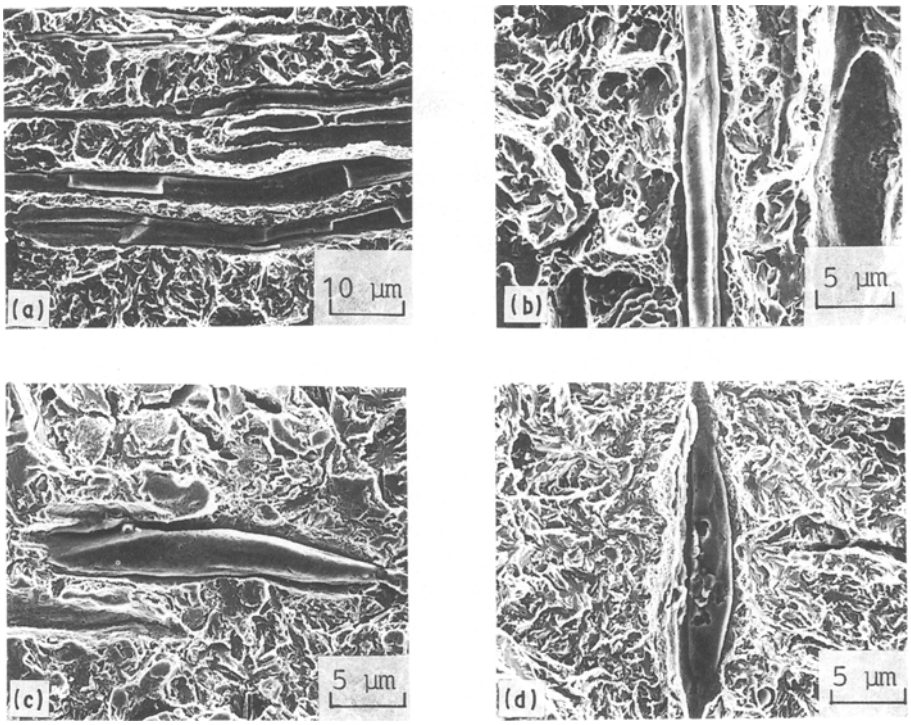

Figure 13 Fracture surface of transverse Charpy U-notch impact test specimens fractured at 77 K (SEM). (a) and (b); T–L and T–T specimens for 98% HRT steel C, respectively. (c) and (d); T–L and T–T specimens for 80% HRT steel C, respectively.

CUN impacted steels at 77 K was then investigated (Fig. 13). As can be seen from this figure, the fracture surface consisted of inclusion voids corresponding to the size of inclusions and brittle fracture facets when the test temperature was decreased.

3.4. Effect of sulphide-inclusion shape on mechanical properties

It has been generally recognized that the affect of inclusions and carbides on ductile fracture caused by microvoid coalescence is classified into three types as shown schematically in Fig. 14. (1) The main crack proceeds by necking of the main crack front and large inclusion voids initiated at the large inclusion sites, resulting in final fracture of the specimen (type 1) [3, 4]. (2) The main crack proceeds by localized shear of internal ligaments between the large inclusion voids initiated at the large inclusion sites, resulting in final fracture of the specimen (type 2) [5]. (3) The main crack proceeds by coalescence of small voids initiated by small inclusions or carbides because of the absence of large inclusion voids at the main crack front, resulting in final fracture of the specimen (type 3).

From the results of fractography in this investigation, the effect of sulphide inclusions on fracture is thought to fall into three stages. (1) Voids are initiated by the fracture of inclusions or by their separation from the matrix. (2) The resulting voids grow somewhat while they are interrupted. (3) Final fracture occurs by localized shear between the voids. Thus, in the present investigation, fracture should be explained by the model of type 2 shown in Fig. 14, therefore, the

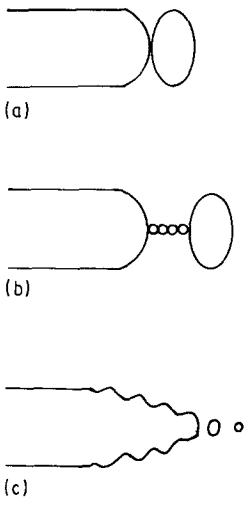

Figure 14 Schematic diagram of three types of fracture model through microvoid coalescence. (a) type 1; (b) type 2; (c) type 3.

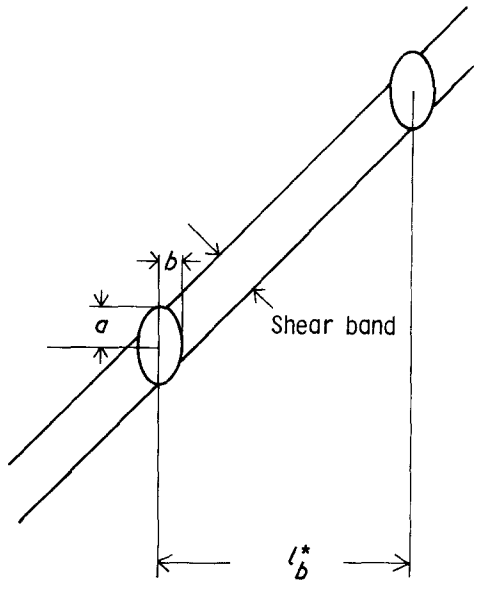

Figure 15 Schematic diagram of shear band joining ellipsoidal holes with semi-axes *a*, *b*, and *c*. The *c* direction is normal to *a* and *b* direction.

important effect of the inclusions on fracture is the shape of the inclusions which determine localized shear. The effect of the sulphide-inclusion shape on fracture is discussed in terms of the model established by McClintock [6–8]. The large inclusion voids may play a predominant role in the development of localized shear bands because a local stress field is formed by large inclusion voids. On the basis of the arguments, the conditions for the development of a shear band were given by (Fig. 15)

$$\frac{1}{\sigma}\left|\frac{d\sigma}{d\varepsilon}\right| < \left(\frac{3}{8}\right)^{1/2} F_b^2 \left(\frac{2b}{l_b^*}\right)^2 \left[\left(\frac{b}{a}\right)^2 + 1\right]^{1/2} \quad (1)$$

where σ is the true stress, ε the true strain; a and b semi-axes of the ellipsoidal holes, l_b^* is the hole spacing in the b direction and F_b the hole growth factor in the b direction. When b/a is approximated by the mean aspect ratio, l/w, and l_b^* is given by Equation 2 [9], Equation 1 becomes

$$l_b^* = \frac{4b}{3f}(1 - f) \quad (2)$$

$$\frac{1}{\sigma}\left|\frac{d\sigma}{d\varepsilon}\right| < kF_b^2 \left(\frac{f}{1-f}\right)^2 \left[\left(\frac{1}{w}\right)^2 + 1\right]^{1/2} \quad (3)$$

where f is the volume fraction of the inclusions and k a constant.

As can be seen from Figs 5 to 7, σ and Table II, f are independent of hot-rolling reduction and the values of $d\sigma/d\varepsilon$ of the steels are also independent of hot-rolling reduction because they are approximated by ε_u. Furthermore, the hole growth factor is thought to be independent of hot-rolling reduction, thus, it is suggested from Equation 3 that decreasing the aspect ratio of the inclusions by decreased hot-rolling reduction decreases the right-hand side of Equation 3 and makes development of a shear band more difficult with a given volume fraction of the inclusions, increasing tensile fracture ductility. The effect of the inclusion shape on CUN impact energies will also be explained by a similar fracture mechanism when the fracture surface consists of large inclusions and small carbide voids, as tensile fracture specimens. The effect cannot, however, be satisfied by the above explanation when the fracture surface consists of large inclusion voids and brittle fracture as the test temperature decreases. In such a case, the effect can be explained by increased σ and decreased $d\sigma/d\varepsilon$ being accompanied by decreased test temperature. That is to say, increasing σ and decreasing $d\sigma/d\varepsilon$ decreased the left-hand side of Equation 3 and makes development of a shear band easier independent of the aspect ratio of the inclusions, resulting in lower CUN impact energy independent of hot-rolling reduction.

The above model can qualitatively explain the affect of the inclusion shape on the mechanical properties in the present investigation. A final explanation is, however, needed for the quantitative relation between shape and development of a localized shear band, unfortunately, this is complex and difficult to establish now. This problem is currently under investigation and its aspects will be reported in future work.

4. Conclusions

Decreased hot-rolling reduction treatments have been applied for improved mechanical properties of quenched and highly tempered low alloy structural steel.

(1) The hot-rolling reduction treatments from 98% $\equiv \times 50$ elongation to 80% $\equiv \times 5$ elongation modified the sulphide-inclusion shape from a stringer to an ellipse independent of the steels.

(2) The decreased hot-rolling reduction treatments significantly increased transverse fracture ductility at similar strength and uniform elongation levels independent of the steels.

(3) The treatments significantly improved the transverse Charpy U-notch (CUN) impact energy in the temperature region which exhibited ductile fracture mode.

(4) The improvement in CUN impact energy was reduced when the temperature decreased and a brittle fracture mode appeared.

(5) The effect of the sulphide-inclusion shape on the mechanical properties is briefly discussed in terms of the model involving large voids nucleated at sulphide-inclusion sites and localized shear bands developed between the large voids.

References

1. W. C. LESLIE, *Trans. Iron Steel Soc.* **2** (1983) 1.
2. Y. TOMITA, *J. Mater. Sci.* **25** (1990) 950.
3. F. A. MCCLINTOCK, "Fracture III" (Academic, New York, 1971) p. 47.
4. J. R. RICE and M. A. JOHNSTON, "Inelastic Behavior of Solids", edited by M. F. Kannineu, W. G. Alder, A. R. Rosenfield and R. I. Jaffee (McGraw-Hill, New York, 1970) p. 61.
5. G. T. HAHN and A. R. ROSENFIELD, *Proc. 3rd. ICF* **3** (1973) 211.
6. H. C. MCCLINTOCK, "Ductility" (ASM, Metal Park, Ohio, USA, 1968) p. 255.
7. T. J. BAKER, K. B. GOVE and J. A. CHARLES, *Met. Technol.* **3** (1976) 183.
8. G. R. SPEICH and W. A. SPITZIG, *Metall. Trans.* **13A** (1982) 2239.
9. "Metal Handbook" (Japan Institute of Metal, Tokyo, 1971) p. 614.

Received 12 May 1989
and accepted 1 February 1990